

## Photoelastic Observation of Spherical Indentation on LiF

V. R. DUMKE

*Departamento de Física, Universidade Federal do Paraná, Caixa Postal 19081, Curitiba, 80.000, PR, Brasil*

Recebido em 02 de setembro de 1982

**Abstract** The application of concentrated load by spherical indenter on LiF monocrystals, produces the characteristic dislocation pattern that is revealed by chemical etching and observed by light microscopy. The residual deformation produces a photoelastic pattern that is composed by stressed regions on  $[110]$  and  $[\bar{1}\bar{1}0]$  directions. Several factors that affect the formation and observation of these patterns are analyzed. An interpretation is presented, based on the geometry of the dislocations produced.

### 1. INTRODUCTION

During the past several years it has become widely recognized that hardness tests represent a useful means of studying various mechanical properties of solids. In polycrystals the impression measurements give the magnitude of the hardness, but in monocrystals the dislocation patterns around an indentation can reveal aspects of the deformation mechanism and plastic flow anisotropies of various crystals. A spherical indenter produces a measure of hardness that is independent of the indenter orientation relative to the crystal lattice, but sensitive to both the orientation of the indented surface and the applied load. Consequently, spherical indentation is particularly interesting to study deformation mechanisms and slip systems.

The dislocation structure of the rosette near an indentation on alkali halides single crystals has been reported by many authors<sup>2,8</sup>. When rock salt structure crystals are loaded on  $\{100\}$  faces through spherical indenters, chemical etching shows a dislocation pattern with arms in both  $\langle 100 \rangle$  and  $\langle 110 \rangle$  directions, corresponding to the operation of  $\{110\}_{45}$  and  $\{110\}_{90}$  slip systems (Fig. 1). The length of the rosette arms in a  $\langle 110 \rangle$  direction is a useful indication of the mechanical strength of the crystal<sup>7</sup>. Nadgorny and Stepanov<sup>1</sup> report that the dislocation pattern is composed by half loops enclosing the indentation,  $\{110\}_{45}$  system, whereas half-loops on  $\{110\}_{90}$  lies on one side only.

However they stand out that the structure of these rosettes may be much more complicated and the motion of dislocations depends on the impurities concentration, magnitude of load and impression velocity.

The present paper indicates the procedures for photoelastic observations and establish a comparison between the stress field and the dislocations patterns around the indentation.

## 2. EXPERIMENTAL

Specimens of LiF, typically  $0,5 \times 0,5 \times 0,2$  cm were prepared by {100} cleavage from a large single crystal block, (Harshaw crystal), and annealed during 24h at  $550^{\circ}\text{C}$  in  $\text{N}_2$  atmosphere to reduce birefringent bands produced by cleavage. The samples were indented with a diamond spherical point, (radius  $18\mu\text{m}$ ), with loads from 10 to 100 gf and loading time of 2 min. After unloading, residual birefringence was observed in optical microscopy, (Wild M-20), using crossed polaroids, following the procedures indicated by Mendelson<sup>9</sup>.

To eliminate spurious birefringences, the sample support was a metallic plate with an aperture, instead of the usual glass plate. In some observations, the analyzer was placed between sample and objective to prevent background stresses produced by the objective lenses. The dislocation distribution around the indentations was revealed by etching with a solution consisting of equal parts of conc. HF and glacial acetic acid, plus 1-vol% of conc. HF saturated with  $\text{FeCl}_3$ <sup>10</sup>.

## 3. OBSERVATIONS

The picture of Fig. 1 shows an indented {100} face of LiF after etching. The four arms in  $\langle 110 \rangle$  directions are composed basically by two rows of edge dislocations, with multiplications between them that decreases gradually from the center to the arm extremity. Observations of the dislocation motion out of the arms due to external stress impulse<sup>2</sup> showed that each row is composed by dislocations with Burgers vectors as indicated in Fig. 1. The four arms in  $\langle 100 \rangle$  directions are composed by screw dislocations and together with the  $\langle 110 \rangle$  arms characterize the spherical indentation. When the indenter is pyramid shaped, its orientation can activate differently the edge,  $\langle 110 \rangle$ , or screw,  $\langle 100 \rangle$ , arms formation<sup>2,4</sup>.

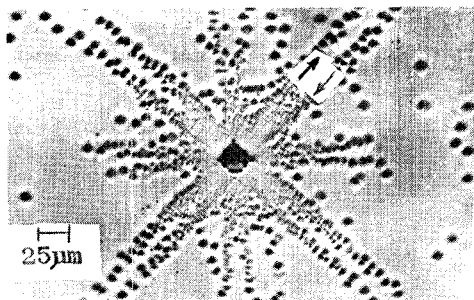


Fig.1 - Dislocation structure of the rosette around a spherical indentation. Burgers vectors indicated according to ref. 2. Load 20 gf

The residual piezobirefringence shown in Fig. 2 is a photograph obtained, before etching, using crossed polaroids which were oriented at right angles to one another and at an angle of  $45^\circ$  with respect to the (010) plane. Only the  $\langle 110 \rangle$  arms present birefringent image. Before indentation, this sample was annealed, after cleavage, at  $600^\circ\text{C}$  during 48h in a  $\text{N}_2$  atmosphere to minimize the effect of background stresses. The photoelastic image is produced by the contribution of the majority of one sign edge dislocations, although the elastic field of an isolated dislocation in LiF, is not sufficient to produce an observable contrast. The indentation produces a pattern that is more prominent between the  $\langle 110 \rangle$  edge rows, where dislocation density is high, vanishing with decreasing intensity from the indentation point. In consequence of the stress magnitudes produced by the indenter, the residual stresses in the material can produce contrast changes in the  $\langle 110 \rangle$  arms of the photoelastic image. An example of this situation is the elastic image showed in Fig. 3, where the loading was done over a nonannealed crystal. The line that crosses all field is a cleavage step left to serve as reference. Residual stresses superimposed with indentation stress produce different rotation on the plane of polarized light forming dark and clear arms. Turning the crystal  $90^\circ$ , the contrast becomes inverted as in Fig. 4. The figures 2, 3 and 4 were obtained with one polaroid over the field diaphragm and the other between sample and objective. However, if the analyzer is fitted above the objective, the pattern becomes modified, since the lens stresses alter the contrast between  $[110]$  and  $[\bar{1}\bar{1}0]$  arms. This is the case of the photoelastic pattern in Fig. 5, that was obtained from the same indentation of Fig. 2, but with the analyzer positioned above the objective. Surface defects were maintained without

polishing to serve as reference.

The photoelastic pattern is not uniform relative to depth, and so there is not a definite thickness that permits a quantitative stress determination. However, the informations are important for indentation studies.

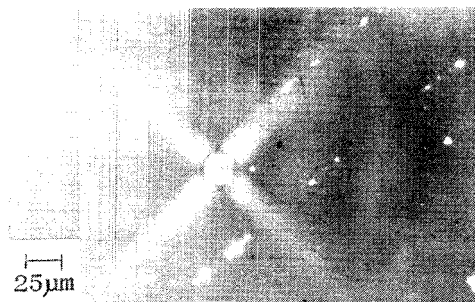


Fig.2 - Photoelastic pattern obtained before etching, showing birefringence bands along  $\langle 110 \rangle$  directions. Load 20 gf

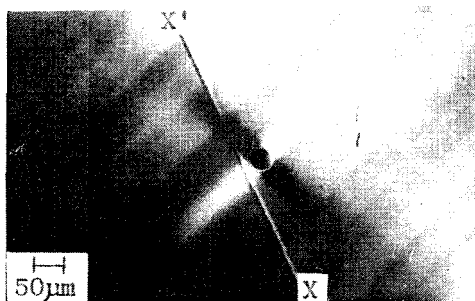


Fig.3 - Photoelastic image of an indentation on a nonannealed crystal. The line  $x-x'$  is a cleavage step left to serve as a reference. Load 20 gf

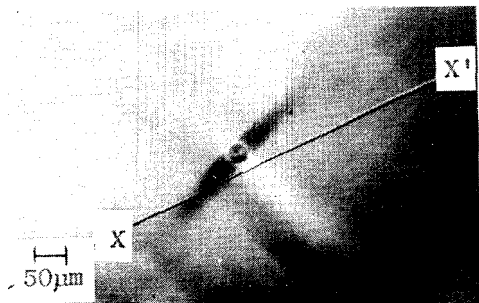


Fig.4 - The same sample of Fig. 3, showing the contrast inversion after  $90^\circ$  turning.

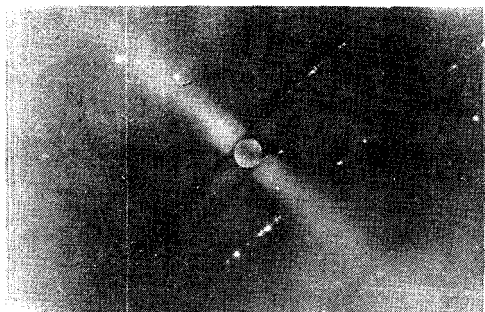


Fig.5 - Photoelastic pattern from the same indentation of Fig.2. Analyzer positioned above the objective.

#### 4. RESULTS AND DISCUSSION

From the comparison between the etch pits and photoelastic patterns, we can conclude that the appearance of birefringence is produced by a dislocation distribution as indicated in Fig. 6. In these conditions, the arms on  $\langle 110 \rangle$  directions are under compression stress, and considering the symmetry and etch pit density, we can assume that the magnitude of the stresses are the same in the four arms. There is no evidence of compression and expansion regions produced by sources approximately in the middle of the arms, as it was proposed in ref. 1 and 2. These sources would produce a pattern as the observed by Mendelson<sup>9</sup>, when a sample is deformed with sources in the central region.

The patterns here observed suggest that dislocations form half-loops that begin on impression region, penetrate in the interior of the crystal, and emerge on several points, producing the arms. The elastic situation permits the hypothesis that there are two different refraction indices, parallel and perpendicular to each arm,  $n_1$  and  $n_2$ , that by Wertheim law result from the difference between  $\sigma_1$  and  $\sigma_2$  stresses, that means

$$(n_1 - n_2) \propto (\sigma_1 - \sigma_2)$$

The optical rotation  $\delta$  produced on the electric field plane by this birefringence will be

$$\delta = C(\sigma_1 - \sigma_2)$$

where C is a proportionality constant that includes the photoelastic constant.

In the absence of other stresses in the sample or in the op-

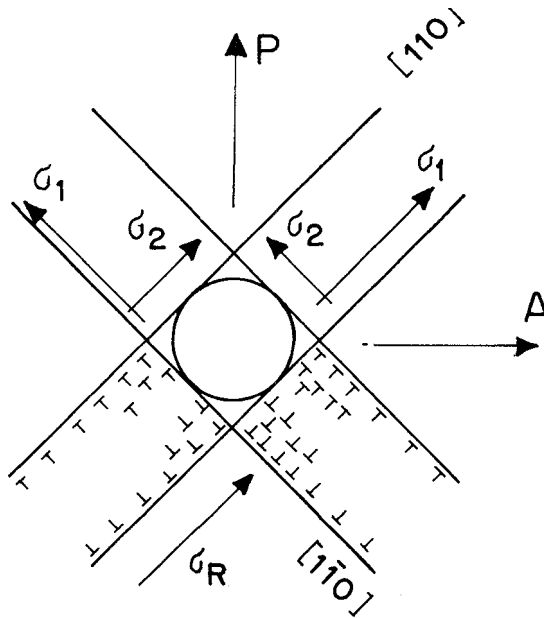


Fig.6 - Scheme of distribution of edge dislocation and principal stresses.

tical system, the rotations produced on the electric field plane that incides on P direction will be due to the difference  $\sigma_1 - \sigma_2$  only. The rotations on  $[\bar{1}10]$  and  $[\bar{1}\bar{1}0]$  arms will present equal magnitudes but with opposite senses. Hence the electric field components along the analyzer direction A are equal, and given by

$$E_A = E_P \sin \delta_{[\bar{h}, k, \ell]}$$

producing arms with equivalent contrasts in the photoelastic image, as observed in Fig. 2. However, existing an uniform residual stress  $\sigma_R$ , for example on  $[\bar{1}10]$  direction, the rotations produced on polarization plane  $\delta_{[\bar{1}10]}$  and  $\delta_{[\bar{1}\bar{1}0]}$  will be

$$\delta_{[\bar{1}10]} = C[(\sigma_1 + \sigma_R) - \sigma_2]$$

and

$$\delta_{[\bar{1}\bar{1}0]} = C[\sigma_1 - (\sigma_2 + \sigma_R)]$$

These rotations will produce different electric field components along direction A, that produce contrasts as observed in Fig.3. Turning the sample  $90^\circ$ , the components contribution become inverted as in Fig.4.

Even in the absence of residual stress in the sample, the objectives can contribute with birefringence that combined with indentation stresses alter the photoelastic pattern as in the case of Fig.5, where the analyzer polaroid was set above the objective. This is the same situation of Fig. 2; however the contribution of residual stresses, present in the objective lenses, alter the contrast on  $[110]$  and  $[\bar{1}\bar{1}0]$  arms.

This effect is produced even by some special objectives for light because of the heating by light radiation. Advantageous conditions for photoelastic observations around indentations are achieved with the analyzer positioned between sample and objective, and avoiding the use of glass plate as sample support.

#### REFERENCES

1. E.M.Nadgorny, A.V.Stepanov, Sov. Phys.- Solid State, Vol. 5, nº 4 732 (1963).
2. V.B.Pariiskii, Phys. Stat. Sol. 19, 525 (1967).
3. M.V.Swain and B.R.Lawn, Phys. Stat. Sol. 35, 909 (1969).
4. J.R.Hopkins, J.A.Miller, J.J.Martin, Phys. Stat. Sol. 19, 591 (1973).
5. D.G.Rickerby, N.H.Macmillan, Mat. Sci. Eng., 40, 251 (1979).
6. M.T. Sprackling, *The Plastic Deformation of Simple Ionic Crystals*, Academic Press (1976).
7. I.V.Gridneva et al., Phys. Stat. Sol. 54, 195 (1979).
8. Yu S.Boyarskaia et al., Kristall und Technik 15, 1179 (1980).
9. S.Mendelson, J.Appl.Phys., 32, 1999 (1961).
10. J.J.Gilman, W.G.Jonston, J.Appl.Phys. 27, 1018 (1956).

#### Resumo

A aplicação de carga concentrada com penetrador esférico em monocristais de LiF, produz o característico padrão de deslocações que é revelado-atraves de ataque químico e observado com microscopia ótica. A deformação residual gera um padrão fotoelástico que se traduz por regiões tensionadas nas direções  $[110]$  e  $[\bar{1}\bar{1}0]$ . São analisados diversos fatores que influem na formação e observação desses padrões bem como sua interpretação com base na geometria das deslocações produzidas.